J|A|C|S
ARTICLES
Published on Web 02/19/2003

Structural Effects on the Barrier Properties of Self-Assembled Monolayers Formed from Long-Chain ω-Alkoxy-*n*-alkanethiols on Copper

G. Kane Jennings,† Tseh-Hwan Yong, Jeffrey C. Munro, and Paul E. Laibinis*,‡

Contribution from the Department of Chemical Engineering, Massachusetts Institute of Technology, Cambridge, Massachusetts 02139

Received February 14, 2002; Revised Manuscript Received November 14, 2002; E-mail: PEL@rice.edu

Abstract: The adsorption of long-chain ω-alkoxy-*n*-alkanethiols [$CH_3(CH_2)_{p-1}O(CH_2)_mSH$; $m = 11, 19, 22$; $p = 18, 22$] onto copper produces self-assembled monolayers (SAMs) that can provide protection against corrosion of the underlying metal substrate. The resulting films are 40−60 Å in thickness and are isostructural with SAMs formed on copper from unsubstituted *n*-alkanethiols. As evidenced by electrochemical impedance spectroscopy (EIS), the barrier properties of these ether-containing SAMs depend on the chain length of the adsorbate and the position of the ethereal unit along the hydrocarbon chain. For SAMs where the ether substitution is farther from the copper surface, the initial coating resistances are similar to those projected for unsubstituted *n*-alkanethiolate SAMs of similar thickness. For SAMs where the ether substitution is nearer to the copper surface ($m = 11$), the resistances are significantly less than those for unsubstituted *n*-alkanethiolate SAMs of similar thickness, reflecting the effect of the molecular structure on the barrier properties of the film. Upon exposure to 1 atm of O_2 at 100% RH, the SAMs become less densely packed as observed by infrared (IR) spectroscopy, and their barrier properties deteriorate as observed by EIS. The rate that the SAMs lose their barrier properties upon exposure to oxidizing conditions is correlated to the strength of intermolecular interactions within the bulk state of the adsorbate.

Introduction

Self-assembled monolayers (SAMs) formed by the chemisorption of *n*-alkanethiols [$CH_3(CH_2)_{n-1}SH$] onto copper[1,2] provide a convenient system for forming densely packed barrier films that protect the underlying metal surface from corrosion. The use of SAMs offers a high level of control over the thickness and chemical composition of the coating by tailoring the synthesis of the adsorbates. This ability enables a detailed, molecular-level examination of the effect of various structural parameters−thickness, packing density, crystallinity, composition−on the level of protection provided by the coating. We[3−5] and others[6−10] have investigated the performance of these alkanethiolate monolayer films as protective coatings on copper and have determined that the SAM can provide a diffusional barrier against the transport of O_2,[3,9] H_2O,[4] and aqueous ions[5] and that cross-linking the films via a robust siloxane network can offer additional methods to improve their level of protection.[6] We have also observed that angstrom-level increases in the thickness of the SAM produce notable enhancements in the protection provided by these films.[3,5] For example, the rate of oxidation of copper−as measured by X-ray photoelectron spectroscopy (XPS)−decreases by 50% for each 4 Å of hydrocarbon thickness in the protecting *n*-alkanethiolate SAM.[3] Furthermore, we have used electrochemical impedance spectroscopy (EIS) to determine that the coating resistances provided by these SAMs with chain lengths of 16−29 carbon atoms increase by 4.2 MΩ cm^2 for each methylene (−CH_2−) in the adsorbate.[5] We have ascribed these dramatic chain-length effects on the barrier properties of the SAMs to the high level of dense packing and crystallinity within the hydrocarbon layer. Specifically, grazing angle infrared (IR) spectroscopy revealed that the ability of these SAMs to maintain their barrier properties upon exposure to oxidizing conditions depends directly on their molecular structure and conformation.[5] SAMs formed from longer-chain thiols form a more stable hydrocarbon lattice that is less affected by increases in surface roughness as induced by oxidation of the underlying metal.

† Current address: Department of Chemical Engineering, Vanderbilt University, Nashville, TN 37235.
‡ Current address: Department of Chemical Engineering, Rice University, Houston, TX 77252-1892.

(1) Laibinis, P. E.; Whitesides, G. M.; Allara, D. L.; Tao, Y.-T.; Parikh, A. N.; Nuzzo, R. G. *J. Am. Chem. Soc.* **1991**, *113*, 7152−7167.
(2) Laibinis, P. E.; Whitesides, G. M. *J. Am. Chem. Soc.* **1992**, *114*, 1990−1995.
(3) Laibinis, P. E.; Whitesides, G. M. *J. Am. Chem. Soc.* **1992**, *114*, 9022−9027.
(4) Jennings, G. K.; Laibinis, P. E. *Colloids Surf., A* **1996**, *116*, 105−114.
(5) Jennings, G. K.; Munro, J. C.; Yong, T.-H.; Laibinis, P. E. *Langmuir* **1998**, *14*, 6130−6139.
(6) Yamamoto, Y.; Nishihara, H.; Aramaki, K. *J. Electrochem. Soc.* **1993**, *140*, 436−443.
(7) Itoh, M.; Nishihara, H.; Aramaki, K. *J. Electrochem. Soc.* **1994**, *141*, 2018−2023.
(8) Itoh, M.; Nishihara, H.; Aramaki, K. *J. Electrochem. Soc.* **1995**, *142*, 3696−3704.
(9) Ishibashi, M.; Itoh, M.; Nishihara, H.; Aramaki, K. *Electrochim. Acta* **1996**, *41*, 241−248.
(10) Feng, Y.; Teo, W.-K.; Siow, K.-S.; Gao, Z.; Tan, K.-L.; Hseih, A.-K. *J. Electrochem. Soc.* **1997**, *144*, 55−64.

10.1021/ja020233l CCC: $25.00

These various studies reveal that thicker SAMs offer greater protection to the underlying copper surface than do thinner SAMs, in terms of both their performance and their lifetimes. On the basis of these studies, the formation of SAMs from longer-chained adsorbates would provide the opportunity to produce thicker films that should provide enhanced barriers to the transport of corrosive agents. In practice, efforts to synthesize *n*-alkanethiols [$CH_3(CH_2)_{n-1}SH$] with $n > 29$ are complicated by lengthy syntheses that are challenged by the poor solubility of the long-chained adsorbates in many common solvents and difficulties in separating synthetic intermediates from starting materials and reaction byproducts. To form SAMs with greater thicknesses and well-defined molecular structures, we have recently described the synthesis and characterization of SAMs formed from long-chain *ω*-alkoxy-*n*-alkanethiols [$CH_3(CH_2)_{p-1}O(CH_2)_mSH$; $m = 11$, $p = 18, 22$; $m = 19$, $p = 18, 22$; $m = 22$, $p = 22$] on gold and copper.[11] The use of an ether linkage for generating long linear chained molecules offers a simpler strategy for coupling two hydrocarbon chains than by formation of C−C bonds. Further, the ethereal oxygen also increases the polarity of the adsorbates and improves their solubility without dramatically affecting the crystallinity of the resulting SAM. Previous structural characterization of shorter-chained *ω*-alkoxy-*n*-alkanethiols [$m = 16$, $p = 1-6$] on gold and silver with IR spectroscopy indicated that the ether linkage provides a local perturbation to chain ordering but that the structural properties of the SAMs are largely insensitive to the ether when it is placed more than two carbons from the outer chain terminus.[12] Miller et al.[13] studied the structural properties for SAMs on gold derived from *ω*-hydroxy-*n*-alkanethiols [$HO(CH_2)_qO(CH_2)_mSH$; $m + q = 13$] that contain an internal ethereal oxygen and showed the ability to form well-defined oriented films from these adsorbates. In this paper, the hydrocarbon chains (particularly in the tail region) are much longer ($p = 18$ or 22). Our results indicate that SAMs as thick as 60 Å can be formed on gold and copper from these *ω*-alkoxy-*n*-alkanethiols and that the SAMs are densely packed and contain a crystalline hydrocarbon backbone that is canted at an average of ∼16° and ∼30° from the surface normal on copper and gold, respectively.[11] On copper, the formation of these SAMs at higher temperature (∼55 °C) from a hydrocarbon solvent resulted in more densely packed films that provided greater barriers against the penetration of aqueous ions than were possible from adsorptions at room temperature. The higher temperatures appear needed to provide sufficient thermal energies to the chains to allow formation of complete films.

In this paper, we examine effects of chain length and molecular structure on the inhibition of corrosion by SAMs formed from the adsorption of *ω*-alkoxy-*n*-alkanethiols onto copper. We have used EIS to determine the coating capacitances and resistances for these SAMs as a function of their exposure to 1 atm of O_2 at 100% relative humidity (RH). We have coupled the EIS results with grazing angle IR spectroscopy to correlate the structure of the SAMs to their barrier properties as a function of their exposure time to the corrosive conditions. By comparing SAMs formed from these long-chained ether-containing adsorbates with those from shorter-chained, unsubstituted *n*-alkanethiols, we are able to relate the effect of the ethereal oxygen on the structure and barrier properties of these monolayer films. Particularly, while the ethereal unit might be a convenient synthetic linker for the synthesis of longer-chained adsorbates, its inclusion may diminish the ability of the film to achieve and maintain dense packing and useful barrier properties. More broadly, this study reveals an intriguing relationship between a bulk property of the adsorbate in the solid state and the effectiveness of derived two-dimensional films as barrier layers.

Results

Properties of *ω*-Alkoxy-*n*-alkanethiols on Copper. We prepared SAMs from *ω*-alkoxy-*n*-alkanethiols on copper by procedures previously detailed to yield densely packed oriented films.[11] In brief, freshly evaporated, polycrystalline copper thin films were prepared on silicon substrates and were transferred immediately under anaerobic conditions to N_2-purged solutions of the *ω*-alkoxy-*n*-alkanethiols (0.5 mM) in isooctane. The assembly was performed at 22 °C for adsorbates with a total carbon chain length ($p + m$) of less than 37 and at 55 °C for the longer-chained adsorbates ($p + m \geq 37$). The higher temperatures were required to provide sufficient thermal motion to the longer chains in the partial films so to allow adsorption of the final thiol adsorbates for complete formation of these thicker SAMs.[11] After adsorption for 1 h, the samples were removed from solution, rinsed sequentially with isooctane and ethanol, and dried in a stream of N_2. The resulting samples exhibited no XPS signals for Cu(II) species. Furthermore, the infrared peak positions of the $\nu_a(CH_2)$, $\nu_s(CH_2)$, and $\nu_a(ROR)$ modes for the freshly prepared SAMs appeared at ∼2919, ∼2851, and ∼1131 cm^{-1}, respectively, and indicated that the films consisted primarily of trans-extended chains that contain few gauche conformers. On the basis of an analysis of the infrared spectra, the intensities of these modes revealed that the hydrocarbon chains cant ∼16° from the surface normal on the copper surfaces.[11,14] The resulting films exhibited wetting properties by water and hexadecane that were similar to those for *n*-alkanethiolate SAMs on copper.[11]

Electrochemical impedance spectroscopy (EIS) provides a method for assessing the protective properties of the SAMs by measuring their resistance against the diffusion of ionic species to the underlying metal surface. EIS has often been used to study the protection provided by polymeric coatings on metals[15,16] and to investigate the barrier properties of SAMs.[17] Figure 1a and b shows Bode magnitude and phase angle plots, respectively, for SAMs formed from $C_{18}OC_{11}SH$, $C_{22}OC_{11}SH$, and $C_{22}OC_{19}SH$ on copper. In Figure 1a for frequencies less than 1 kHz, the log of the impedance magnitude increases linearly (slope of 1) with decreasing log frequency. This behavior

(11) Jennings, G. K.; Yong, T.-H.; Munro, J. C.; Laibinis, P. E. *Langmuir*, submitted.
(12) Laibinis, P. E.; Bain, C. D.; Nuzzo, R. G.; Whitesides, G. M. *J. Phys. Chem.* **1995**, *99*, 7663−7676.
(13) Sinniah, K.; Cheng, J.; Terretaz, S.; Reutt-Robey, J. E.; Miller, C. J. *J. Phys. Chem.* **1995**, *99*, 14500−14505.
(14) The cant of ∼16° determined by reflectance IR spectroscopy for the SAMs derived from *ω*-alkoxy-*n*-alkanethiols on polycrystalline copper surfaces[11] is similar to values determined for SAMs formed from unsubstituted *n*-alkanethiols on polycrystalline copper surfaces by IR (∼13°)[1] and on Cu(111) surfaces by NEXAFS (∼12.2°) (Rieley, H.; Kendall, G. K. *Langmuir* **1999**, *15*, 8867−8875). The polycrystalline copper surfaces have a predominant (111) texture.[1]
(15) Bellucci, F.; Kloppers, M.; Latanision, R. M. *J. Electrochem. Soc.* **1991**, *138*, 40−48.
(16) Mitton, D. B.; Latanision, R. M.; Bellucci, F. *J. Electrochem. Soc.* **1996**, *143*, 3307−3316.
(17) Finklea, H. O. Electrochemistry of Organized Monolayers of Thiols and Related Molecules on Electrodes. In *Electroanalytical Chemistry*; Bard, A. J., Rubinstein, I., Eds.; Marcel Dekker: New York, 1996; Vol. 19, pp 109−335.

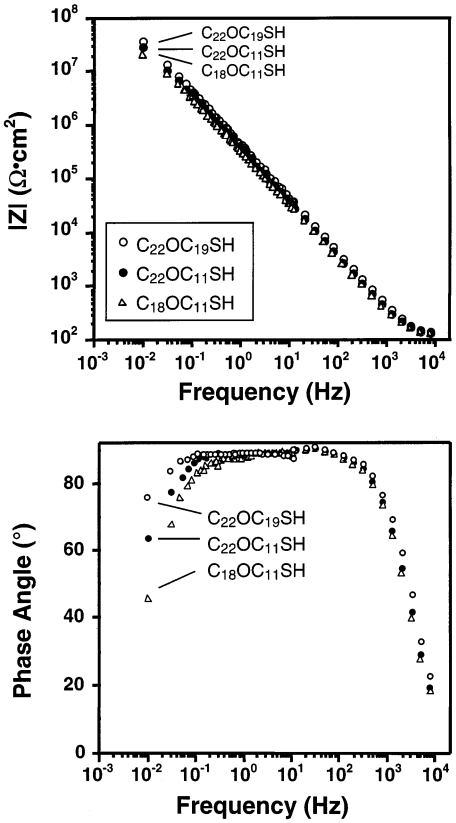

Figure 1. (a) Bode magnitude and (b) phase plots for copper protected with SAMs of $C_{18}OC_{11}SH$, $C_{22}OC_{11}SH$, and $C_{22}OC_{19}SH$ in oxygenated 50 mM Na_2SO_4 (aq).

indicates that the films behave primarily as a low dielectric layer that separates the corrosive solution from the underlying copper. At the lowest frequencies in Figure 1, the impedance of the coating capacitance becomes sufficiently large that the resistance of the coating begins to control the response. This transition is illustrated best in Figure 1b in which the phase angle decreases from 90°—a value characteristic of capacitive behavior—at the lowest frequencies. The decrease in phase angle is most pronounced for the $C_{18}OC_{11}S$-SAM and least for the $C_{22}OC_{19}S$-SAM, suggesting that the thicker SAM provides a less permeable barrier to the diffusion of ions.

Modeling the impedance data for an *n*-alkanethiolate SAM on copper with an appropriate equivalent circuit model[3] enables estimation of the capacitance and resistance of a coating. Because the SAM can be described as a low dielectric medium separating two parallel conductors (the metal and the solution), the capacitance of the coating should decrease as the coating thickness is increased. Figure 2 shows that the inverse capacitance of the film is linearly related to the chain length (no. of carbons + no. of oxygens) of the adsorbate for coatings derived from both unsubstituted *n*-alkanethiols and *ω*-alkoxy-*n*-alkanethiols adsorbed on copper. That these data sets lie approximately on the same line suggests that SAMs formed from the ether-linked thiols are similar in dielectric properties to those from the *n*-alkanethiols and that the effective thickness of the SAM can be increased incrementally by increasing the adsorbate chain length from 8 to 45. The thickness trends inferred from these capacitance data are consistent with our results from X-ray photoelectron spectroscopy (XPS) in which the Cu ($2p_{3/2}$) photoelectron intensity from the underlying substrate decreased

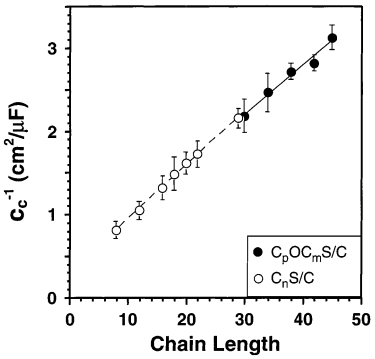

Figure 2. Inverse capacitance of SAMs of C_nSH and C_pOC_mSH on copper in oxygenated 50 mM Na_2SO_4 (aq). The lines are least-squares fits to the data and have slopes that correspond to dielectric permittivities of ~2.16 and ~2.35 for the C_nSH and C_pOC_mSH SAMs, respectively.

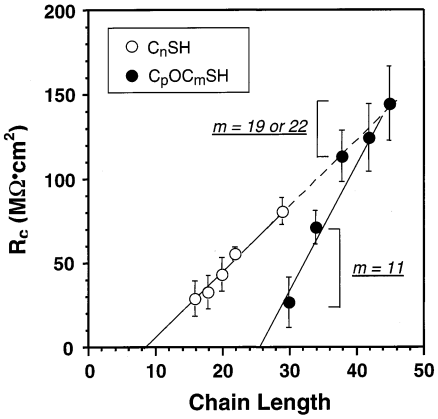

Figure 3. The effect of chain length on the coating resistance for SAMs prepared from C_nSH and C_pOC_mSH on copper. Coating resistances were determined by fitting the impedance data to an equivalent circuit consisting of a solution resistance in series with a parallel combination of coating resistance and coating capacitance.[5] The lines are least-squares fits to the data.

exponentially with increased chain length at similar rates for both adsorbed *n*-alkanethiols and *ω*-alkoxy-*n*-alkanethiols.[11] The dielectric permittivity (ϵ) of the coatings can be estimated from the slope of the line,[5] to give values for ϵ of ~2.16 for the purely hydrocarbon SAMs and ~2.35 for the ether-substituted SAMs. These permittivities agree well with values of 2.3 determined for polyethylene[18] and 2.1 measured for C_nSH ($n = 16, 18$) on gold with surface plasmon resonance.[19]

Figure 3 shows the coating resistances for SAMs on copper derived from both unsubstituted *n*-alkanethiols and *ω*-alkoxy-*n*-alkanethiols as a function of the chain length of the adsorbate. As we have previously shown,[5] the coating resistances for SAMs of C_nSH on copper increase linearly with chain length for $n \geq 16$ with a slope of 4.2 MΩ cm² for each incremental methylene unit. That the best-fit line through the alkanethiol data intersects the *x*-axis at $n \cong 10$ may reflect the minimum chain length required to achieve a region within the SAM that is sufficiently crystalline to impede the transport of corrosive species to the underlying copper surface.[5] For SAMs formed from *ω*-alkoxy-*n*-alkanethiols on copper, the coating resistance also increases with chain length, but these data are not a simple extension of the linear behavior of the C_nSH-systems as was the case for the capacitance data (Figure 2). In fact, the coating resistances

(18) Lanza, V. L.; Herrman, D. B. *J. Polym. Sci.* **1958**, *28*, 622−625.
(19) Peterlinz, K. A.; Georgiadis, R. *Langmuir* **1996**, *12*, 4731−4740.

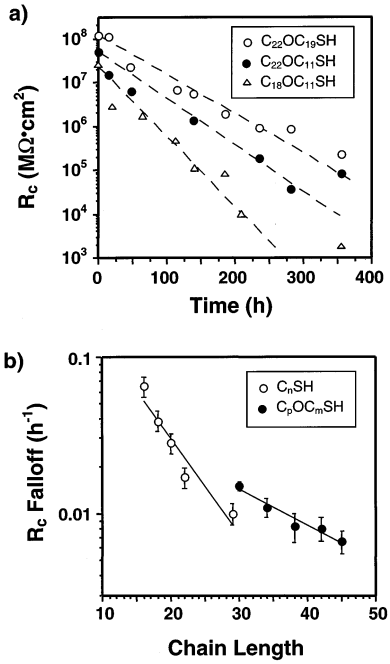

Figure 4. (a) Time dependence of the coating resistance for SAMs formed from $C_{18}OC_{11}SH$, $C_{22}OC_{11}SH$, and $C_{22}OC_{19}SH$ on copper upon exposure to 1 atm of O_2 at 100% RH. The lines are least-squares fits to the data and were constrained to intersect the initial ($t = 0$) data point. (b) Relationship between the rate of coating resistance falloff (determined from Figure 4a) for SAMs of C_nSH and C_pOC_mSH on copper and the chain length of the adsorbate that forms the coating. The lines represent least-squares fits to the data. From the slope of the lines, the incremental chain lengths that are required to reduce the coating resistance by 50% are approximately 5 and 13 $-CH_2-$ units for the C_nSH and C_pOC_mSH systems, respectively.

for SAMs formed from $C_{18}OC_{11}SH$ (chain length = 30) and $C_{22}OC_{11}SH$ (chain length = 34) are significantly smaller than those expected on the basis of a linear extrapolation of the data for C_nS-films, while resistances for SAMs formed from C_pOC_m-SH ($m + p \geq 37$) agree with those projected for a C_nS-SAM of similar chain length. The best-fit line through the data intersects the *x*-axis at a chain length of ~25, considerably higher than that ($n \cong 10$) for SAMs formed from C_nSH.

Properties of SAMs upon Exposure to 1 atm of O_2 at 100% RH. Exposure of SAMs formed from ω-alkoxy-*n*-alkanethiols on copper to 1 atm of O_2 and 100% relative humidity (RH) at room temperature caused a degradation in the protective properties of the films. Figure 4a shows the coating resistance (R_c) for SAMs of $C_{18}OC_{11}SH$, $C_{22}OC_{11}SH$, and $C_{22}OC_{19}SH$ on copper as a function of exposure time to these oxidizing conditions. While the coating resistance for each SAM decreases exponentially with increased exposure, the thinnest SAM ($C_{18}OC_{11}SH$) exhibits the most rapid loss of coating resistance. Sequential increases in the outer chain length by four methylene units ($C_{22}OC_{11}SH$) and the inner chain length by eight methylene units ($C_{22}OC_{19}SH$) each result in films that exhibit slower losses in their coating resistance. From data such as those in Figure 4a, we determined the rate of coating resistance falloff for SAMs formed from the various ω-alkoxy-*n*-alkanethiols and compared them to data obtained by us[5] from unsubstituted *n*-alkanethiolate SAMs (Figure 4b). The data for both systems show a similar trend in that the thicker films are the more effective in maintaining their barrier properties upon exposure to 1 atm of O_2 at 100% RH. Nevertheless, the slopes of the ether and non-ether data sets in Figure 4b are distinctly

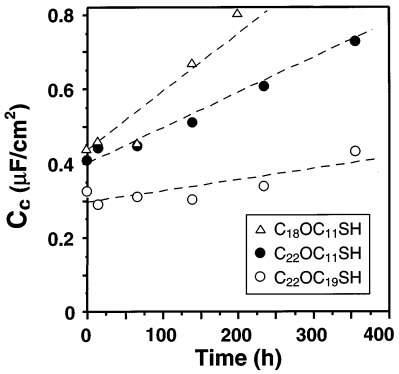

Figure 5. Time dependence of the coating capacitance (C_c) for SAMs formed from $C_{18}OC_{11}SH$, $C_{22}OC_{11}SH$, and $C_{22}OC_{19}SH$ on copper upon exposure to 1 atm of O_2 at 100% RH. The lines serve as guides to the eye.

different and indicate that each additional methylene added to an unsubstituted *n*-alkanethiolate SAM results in a greater reduction in the rate of R_c falloff than one added to an ω-alkoxy-*n*-alkanethiolate SAM. Specifically, a decrease in the rate of R_c falloff by 50% requires the addition of only 5 methylene units to the unsubstituted thiol and roughly 13 methylene units to the ether-substituted thiol that forms the SAM.

Figure 5 shows capacitances for SAMs of $C_{18}OC_{11}SH$, $C_{22}OC_{11}SH$, and $C_{22}OC_{19}SH$ on copper after various exposure times to 1 atm of O_2 at 100% RH. Increases in capacitance can correspond to the uptake of water or ions in the coating and/or the SAM becoming effectively thinner (vide infra). For these SAMs in Figure 5, the values of the coating capacitance (C_c) change little (if any) over the first ~70 h of exposure; however, R_c (Figure 4a) for all of these SAMs decreases by nearly an order of magnitude over a similar time of exposure. The decrease in R_c is probably due to slight structural perturbations in the film caused by oxidation of the underlying copper and subsequent roughening of the surface. After 70 h, the C_c values of the $C_{18}OC_{11}S$- and $C_{22}OC_{11}S$-SAMs increase more dramatically, suggesting the formation of larger defects within the coating that may serve as paths for ionic conduction. The more subtle change in C_c for the $C_{22}OC_{19}S$-SAM over the entire exposure may reflect the greater structural integrity of this thicker film.

In previous work, we used grazing angle IR spectroscopy to monitor the structural properties for SAMs derived from C_nSH ($n = 16$, 22, and 29) on copper upon exposure to 1 atm of O_2 at 100% RH.[5] Our results suggested that the SAMs become less densely packed and less crystalline upon exposure to these conditions but that the thicker SAMs ($n = 29$) exhibited a slower transition to the less crystalline state. We also observed that increases in the average cant of the adsorbates were concurrent with increases in the capacitance of the SAMs, both results signaling the transformation to an effectively thinner film. Figure 6 shows grazing angle IR spectra of the C−H and R−O−R stretching regions for SAMs formed from $C_{22}OC_{11}SH$ (Figure 6a) and $C_{22}OC_{19}SH$ (Figure 6b) on copper after various exposures to 1 atm of O_2 at 100% RH. The spectral changes observed for the $C_{22}OC_{11}S$-SAM are similar to those observed for the $C_{18}OC_{11}S$-SAM (not shown), while changes for the $C_{22}OC_{19}S$-SAM are typical of those exhibited by coatings of the longer chained adsorbates ($C_{18}OC_{19}SH$ and $C_{22}OC_{22}SH$). For the shorter-chained $C_{22}OC_{11}S$-SAM (Figure 6a), increases in the intensities of the $\nu(CH_2)$ modes and a reduced intensity of the ν_a(ROR) mode upon increased exposure suggest that the

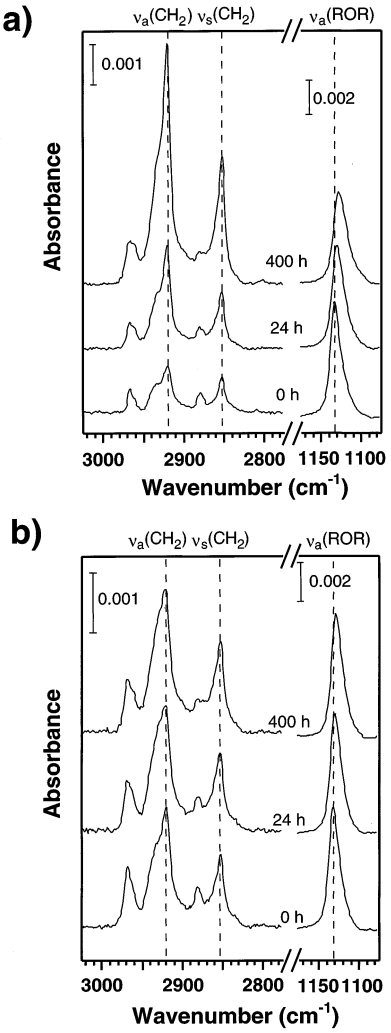

Figure 6. Grazing incidence polarized infrared spectra of the C−H stretching region for SAMs of (a) $C_{22}OC_{11}SH$ and (b) $C_{22}OC_{19}SH$ on copper before and after exposure to 1 atm of O_2 at 100% RH for various times. The dashed lines represent the positions of the primary modes for a trans-extended monolayer with no gauche defects: $\nu_a(CH_2) = 2918$ cm^{-1}, $\nu_s(CH_2) = 2851$ cm^{-1}, and $\nu_a(ROR) = 1132$ cm^{-1}. The spectra have been offset vertically for clarity.

adsorbates within the SAM become more canted and less densely packed after exposures of 24 and 400 h, consistent with the increase in capacitance for this film (Figure 5). The peak positions for the $\nu(CH_2)$ modes remain at or near their initial values—$\nu_a(CH_2)$ at ~2919 cm^{-1} and $\nu_s(CH_2)$ at ~2851 cm^{-1}—during the 400 h exposure, suggesting that the hydrocarbon maintains its primarily trans-extended structure; however, the ν_a(ROR) peak becomes broadened and shifts from 1132 to 1127 cm^{-1}, indicating a less crystalline local environment near the ether substitution[11] after 400 h of exposure. While the methyl stretching modes provide no direct information about the cant of the adsorbates, they are useful for assessing the structural heterogeneity at the outermost region of the SAM. During the exposure, both the $\nu_a(CH_3)$ and the $\nu_s(CH_3)$ modes become broadened with the $\nu_a(CH_3)$ increasing in intensity and the $\nu_s(CH_3)$ decreasing in intensity. These changes are consistent with an increased average tilt of the adsorbates within the SAM and the evolution of a more heterogeneous methyl environment at the surface. Clearly, exposure to the corrosive conditions causes major structural changes in the $C_{22}OC_{11}S$-SAM.

In contrast to the $C_{22}OC_{11}S$-SAM on copper, the $C_{22}OC_{19}S$-SAM exhibits less dramatic structural changes during exposure to 1 atm of O_2 at 100% RH for 400 h (Figure 5b). The relatively constant intensities of the $\nu_a(CH_2)$, $\nu_s(CH_2)$, and ν_a(ROR) modes indicate that the adsorbates within the SAM remain densely packed during the 400 h exposure; however, the broadening of the methylene modes suggests some loss in crystallinity. In comparing Figure 6a and b at 400 h exposure, it is evident that the addition of eight methylene units to the bottom portion of the SAM significantly enhances its ability to maintain its structure. The better ability for the $C_{22}OC_{19}S$-SAM to maintain its structure agrees well with its relatively constant capacitance, and both suggest that the effective thickness of the film does not change dramatically through a 400 h exposure to the corrosive conditions. Similar to the $C_{22}OC_{11}S$-SAM, the peak positions of the $\nu_a(CH_2)$ and $\nu_s(CH_2)$ modes for the $C_{22}OC_{19}S$-SAM remain essentially constant during the exposure, while that for the ν_a(ROR) mode decreases from 1131 to 1128 cm^{-1}, indicating a local loss of crystallinity near the ether substitution. The outer surface of the SAM becomes more heterogeneous during the exposure, as evidenced by broadening of both the $\nu_a(CH_3)$ and the $\nu_s(CH_3)$ modes.

Discussion

Effect of Ether Substitution on Barrier Properties. The results of Figures 1−6 consistently demonstrate that the chain length of the adsorbates forming the SAM significantly impacts the properties of the resulting films. The capacitance results in Figure 2 illustrate that effectively thicker SAMs can be formed on copper by use of long-chain *ω*-alkoxy-*n*-alkanethiols than are presently available from *n*-alkanethiols and that their thickness scales with the chain length of the adsorbates. The incorporation of the ether unit shows little variation from that expected for addition of a methylene unit, suggesting that this linkage is a relatively innocent addition to the SAMs in terms of its effect on the overall thickness and capacitance of the film. While capacitance provides a measure of the bulk permeability of the SAMs toward simple ionic species, resistance measurements are more sensitive to the fine structural details of the film. In contrast to the capacitance data, the coating resistances for the long-chain *ω*-alkoxy-*n*-alkanethiols are not linear extensions of the unsubstituted *n*-alkanethiol data (Figure 3). The coating resistances for SAMs of *ω*-alkoxy-*n*-undecanethiols ($C_{18}OC_{11}SH$ and $C_{22}OC_{11}SH$) are significantly less than those expected for *n*-alkanethiols of similar chain length, while resistances for the longer-chained ether-containing thiols ($C_{18}OC_{19}SH$, $C_{22}OC_{19}SH$, and $C_{22}OC_{22}SH$) are much closer to a linear extrapolation of the C_nSH data. These data may be rationalized by considering the likely locations of gauche conformations within the hydrocarbon SAM. Hautman and Klein used molecular dynamics simulations to study the structure of SAMs from $C_{16}SH$ on gold and determined that gauche defects are concentrated near the chain termini.[20,21] In contrast with the tendency of polymethylene chains to adopt trans-extended conformations, ethereal units induce a preference for adoption of gauche conformers in the C−C bonds adjacent to an ether unit.[22] In one study of these issues in a SAM, Laibinis et al. used IR spectroscopy of ether-containing SAMs on gold and silver and concluded that the presence of an ethereal oxygen

(20) Hautman, J.; Klein, M. L. *J. Chem. Phys.* **1989**, *91*, 4994−5001.

along the hydrocarbon chain of a SAM causes a local disordering to the chain and an increase in the population of gauche conformations in the SAM.[12] Their results also indicated that SAMs formed from $CH_3O(CH_2)_mSH$ on silver were significantly less crystalline for $m = 8$ and 11 than for $m = 16$.

On the basis of these perturbations, the structure for the *ω*-alkoxy-*n*-alkanethiolate SAMs in the present paper is likely to include regions of reduced crystallinity near the metal surface, near the ether substitution, and near the outer portion of the SAM at the air interface. Regions of higher crystallinity would be localized in methylene units sufficiently separated from regions disposed to local disordering and preferences for gauche conformers (such as those near a chain end or an ether unit), with the possibility that adjacent regions of order or disorder could work cooperatively to overcome the structural preference of one region when in isolation. For example, nearby regions of disorder may work together so that an intervening hydrocarbon chain may become less crystalline, while neighboring stretches of trans-extended methylene units may decrease the ability of a connecting ether unit to induce local gauche conformers. For the SAMs formed from *ω*-alkoxy-undecanethiols, the close proximity of the lower and middle regions of higher gauche density may result in a less ordered layer of hydrocarbon between the ether linkage and the metal surface. For these SAMs, only the thicker hydrocarbon layer above the ether linkage could be expected to achieve high levels of conformational order. In Figure 3, the similar R_c values for SAMs formed from $C_{18}OC_{11}SH$ and $C_{18}SH$ and for SAMs formed from $C_{22}OC_{11}SH$ and $C_{22}SH$ SAMs provide support for this hypothesis of a more ordered top layer and a less ordered bottom layer. For SAMs where the ether substitution is significantly further away from the copper surface, a higher degree of structural order could be expected for the contiguous hydrocarbon portion between the ether linkage and the metal surface. In Figure 3, the similarity between the R_c values for SAMs formed from $C_pOC_{19,22}SH$ and those projected for SAMs formed from *n*-alkanethiols of the same chain length—that is, $n = m + p + 1$—suggests adoption of similar structures.

We previously hypothesized that the eventual oxidation of copper upon exposure to 1 atm of O_2 at 100% RH results in a nanoscale surface roughening that promotes a transition within the SAM to a less organized structure and negatively impacts its barrier properties.[5] Figure 4b indicates that the rate of coating resistance falloff for an *ω*-alkoxy-*n*-alkanethiolate SAM is faster than that for an unsubstituted *n*-alkanethiolate SAM of similar chain length. Furthermore, the addition of incremental methylene units to the ether-linked adsorbates results in a smaller reduction in the R_c falloff than a similar addition to unsubstituted *n*-alkanethiols. In other words, the rate of R_c falloff is not solely dependent on film thickness. If the structural stability of the monolayer affects its barrier properties, then the rate of R_c falloff should depend on the strength of the intermolecular interactions between the molecules that comprise the film. A sensitive, albeit qualitative, metric of these solid-state interactions is the temperature where an ordered system transitions to a less ordered (liquidlike) state. To test this hypothesis, we plot the rate of R_c falloff in Figure 7 as a function of the melting temperature (T_{melt}) of the parent compound for SAMs formed from C_nSH and C_pOC_mSH. For a constant chain length, the ether-substituted thiols have lower melting points than the unsubstituted *n*-alkanethiols due to the perturbation of interchain packing imposed by the ethereal substitution.[12] Figure 7 shows that the rate of R_c falloff decreases exponentially as T_{melt} increases for both *n*-alkanethiols and *ω*-alkoxy-*n*-alkanethiols and that the data for the two systems exhibit a similar correspondence with T_{melt}. This result across these two systems suggests that the effectiveness of a SAM to maintain its barrier properties (R_c) depends on the strength of the intermolecular interactions within the monolayer and its ability to form a crystalline structure rather than simply on the thickness of the SAM. The SAMs comprising molecules that achieve a greater level of intermolecular interaction are superior in maintaining their structural integrity through exposure to the examined oxidizing conditions.

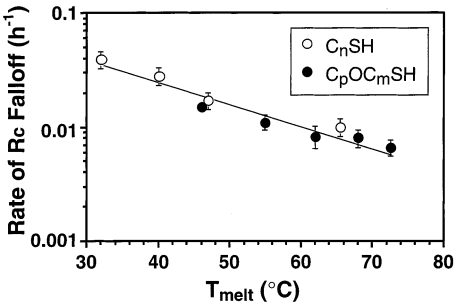

Figure 7. Relationship between the rate of coating resistance falloff for SAMs of C_nSH and C_pOC_mSH on copper from Figure 4b and the melting point of the adsorbate. The line is a least-squares fit to the data.

Mechanism for Breakdown in SAM Protection. Upon exposure of SAM-coated copper to 1 atm of O_2 at 100% RH, the adsorbates within the SAM undergo modest ($C_{22}OC_{19}SH$) or extensive ($C_{22}OC_{11}SH$) structural transformations (Figure 6), and the capacitance of the SAM increases (Figure 5), while its resistance decreases (Figure 4). Increases in the capacitance of the SAM can be related to a decrease in its thickness or an increase in its dielectric permittivity due to the uptake of aqueous species within the film or at defect sites. If increases in capacitance are solely due to a reduction in thickness of the SAM resulting from an increased average cant of the adsorbates (either by loss of adsorbed material or by local surface roughening), then an estimation of the change in SAM thickness based on capacitance measurements should be similar to that estimated from the $\nu(CH_2)$ intensities in IR spectroscopy. For a $C_{22}OC_{11}S$-SAM exposed to 1 atm of O_2 at 100% RH for 350 h (Figure 5), the increase in capacitance would correspond to a

(21) The structural picture that emerges from the coating resistances obtained by EIS for *n*-alkanethiolate SAMs on copper (Figure 3) is that the terminal parts of the chain—that is, that near the copper surface and that near the SAM/air(solution) interface—contain a total of roughly 10 disordered methylene units and that any additional methylene units in the alkyl chain form a densely packed, highly trans-extended region within the interior of the SAM.[5] This perspective is somewhat different from interpretations of vibrational spectra for SAMs that suggest shorter chain lengths ($n \leq 12$) produce SAMs with a high density of gauche conformers—$\nu_a(CH_2)$ appears at 2920−2923 cm^{-1}—and longer chain lengths ($n \geq 16$) produce SAMs with a trans-extended conformation—$\nu_a(CH_2)$ appears at ~2919 cm^{-1}. A simplified misinterpretation of the spectral results is that chain lengths (*n*) less than 12 produce disordered SAMs and lengths greater than 16 produce fully crystalline or ordered SAMs. This interpretation of completely trans-extended structures for the longer-chained adsorbates (based primarily on the position of the $\nu_a(CH_2)$ peak rather than on its shape and heterogeneity) excludes suggestions that gauche conformers accumulate at the chain ends[20] and that the structure along the chain might not be homogeneous. The suggestion from EIS of a coexistence of disordered and crystalline regions within a SAM is not incompatible with IR spectra of *n*-alkanethiolate SAMs;[1] however, EIS suggests a greater amount of disorder. This difference may reflect an ability by EIS to differentiate better between finer distinctions in structure and to probe lower levels of disorder, particularly as they affect barrier properties.

(22) Miwa, Y.; Machida, K. *J. Am. Chem. Soc.* **1989**, *111*, 7733−7739 and references therein.

decrease in thickness of ~40% from the initially prepared SAM. The increased intensity of the $\nu(CH_2)$ modes (Figure 6a) over the 400 h exposure to the oxygenated conditions suggests that the average cant of the film has increased from 17° to 39°, corresponding to a decrease in thickness of only ~20%. Because capacitance measurements suggest a greater reduction in film thickness than IR spectroscopy, the increase in capacitance is at least partially due to an increase in the dielectric permittivity (ϵ_{SAM}) of the coating. Whether the increase in ϵ_{SAM} is due to an uptake of aqueous species throughout the SAM or their accumulation at specific defect sites within the SAM cannot be unequivocally determined from these results. Such a large increase in film capacitance (~40%) is not expected to result solely from the equilibrium uptake of electrolyte throughout the film, as the solubility of water in these films is extremely low. Therefore, defects that form within the SAM upon exposure to 1 atm of O_2 at 100% RH likely become filled with electrolyte during the EIS measurement, increasing the capacitance of the films. Nevertheless, none of our experimental evidence suggests the existence of true pinholes defined as bare areas of the metal surface that are in direct contact with the electrolyte. For example, we observed no Warburg impedance in our EIS spectra that would be characteristic of solution/metal contact at pores in the film for these SAMs, even after prolonged exposure to 1 atm of O_2 at 100% RH. The presumed absence of pinholes is attributed to the tendency of the long, flexible hydrocarbon chain in the adsorbates to form van der Waals interactions with neighboring molecules and reduce the size of any defects that may form.

The results in Figure 7 provide support for the proposed mechanism of film deterioration discussed above. After formation of the SAM and subsequent exposure to 1 atm of O_2 at 100% RH, oxygen diffuses through the film and reacts to convert the copper metal to Cu(I) and eventually Cu(II) oxide and thiolates to sulfonates.[3,23] The oxidation of copper likely proceeds with roughening of the underlying substrate that effectively melts the crystalline lattice of the adsorbed film and increases its density of defects. These structural changes within the SAMs were revealed in the data from IR spectroscopy and wetting measurements. Upon exposure to 1 atm of O_2 at 100% RH, the IR spectra for these SAMs (Figure 6) displayed a broadening of the $\nu(CH_2)$ and $\nu(CH_3)$ peaks, an increase in the intensity of the $\nu(CH_2)$ modes (for most SAMs), and a slight shift in the peak positions of the $\nu_a(CH_2)$ and $\nu_s(CH_2)$ modes to higher wavenumbers. These changes are indicative of a transition from a purely crystalline film to a more heterogeneous one with a reduced packing density. In a similar manner, the SAMs display lower contact angles of hexadecane[4] and greater contact angle hysteresis of water[3] upon exposure to oxidizing conditions, indicating the formation of a more chemically heterogeneous and roughened surface. When the SAM-coated samples are removed from the oxidizing conditions and exposed to an aqueous solution (during EIS measurement), penetration of water and electrolyte into the defects of the SAMs causes a reduction in the resistance and an increase in the capacitance of the SAM. The chain length trends described here demonstrate that SAMs formed from adsorbates that exhibit greater intermolecular interaction in their bulk state (Figure 7) possess enhanced stability against structural perturbations such as those induced by oxidation of the copper substrate. In support of these results, Zamborini and Crooks[24] and others[25,26] have revealed the importance of intermolecular interactions on film stability by reporting that SAMs on gold derived from thiols with intermolecular hydrogen-bonding capabilities are more stable to repeated oxidative electrochemical cycling and exposure to elevated temperatures.

The suggestion from the present work is that the design of molecular barrier coatings with extended lifetimes requires structures able to provide good two-dimensional packing and incorporate functionalities or species able to provide strong intermolecular interactions. The use of higher processing temperatures for achieving formation of such densely packed, organized films may provide a particular benefit for generating barrier films that are able to maintain their solid-state characteristics more effectively at a lower operating temperature. In essence, a higher thermal energy can be beneficial for allowing free movement of molecules during their organization of a barrier film, while a lower thermal energy during operation is useful for restricting the molecular motion within a SAM and maintaining its desired supramolecular state.

Conclusions

The protection of copper by thiol-based self-assembled monolayers (SAMs) is sensitive to the chemical composition and molecular structure of the barrier film. The use of long-chain *ω*-alkoxy-*n*-alkanethiols provides a convenient strategy for preparing relatively thick SAMs on copper, with thicknesses of 40−60 Å by a single adsorption step. The performances of these films as barrier layers depend on the chain length of the adsorbate and the position of the ethereal unit along the hydrocarbon chain. For SAMs prepared from *ω*-alkoxy-undecanethiols ($C_{22}OC_{11}SH$ and $C_{18}OC_{11}SH$), the measured coating resistances are significantly lower than those expected for unsubstituted *n*-alkanethiols of similar chain length, consistent with a structure containing a less crystalline region near the base of the SAM. In contrast to these SAMs, those prepared from *ω*-alkoxy-*n*-nonadecanethiols and *ω*-alkoxy-*n*-docosanethiols exhibit higher initial resistances (up to 150 MΩ cm^2) and are superior in maintaining their structural properties upon exposure to corrosive conditions. In these SAMs, the ether unit is positioned at least 18 carbon units from a chain end to limit its disordering influence on the SAM. The results illustrate that the ability of a SAM to maintain its barrier properties during prolonged exposure to these conditions is related to the strength of intermolecular interactions within the SAM rather than simply its thickness. The data suggest that the design of barrier coatings requires a selection of adsorbates that can geometrically achieve dense packing and high crystallinity and are energetically able to maintain these structural properties, where their melting points

(23) Schoenfisch and Pemberton have shown that (1) thiolate SAMs on gold convert to sulfonates upon exposure to ozone-containing air, (2) the sulfonates are not easily removed from the substrate, and (3) the barrier properties of the films are not affected by this oxidation (see: *J. Am. Chem. Soc.* **1998**, *120*, 4502−4513.) As we observe no loss of adsorbate from the SAMs on copper upon their exposure to the aqueous electrolyte during impedance measurements,[5] the oxidation of thiolates to sulfonates is not expected to account completely for the exponential decrease in the resistance of these films.

(24) Zamborini, F. P.; Crooks, R. M. *Langmuir* **1998**, *14*, 3279−3286.
(25) Tam-Chang, S.-W.; Biebuyck, H. A.; Whitesides, G. M.; Jeon, N.; Nuzzo, R. G. *Langmuir* **1995**, *11*, 4371−4382.
(26) Clegg, R. S.; Reed, S. M.; Hutchison, J. E. *J. Am. Chem. Soc.* **1998**, *120*, 2486-2487.

can provide a useful comparative meter for their likely performance.

Experimental Section

Materials and Synthesis. Copper shot (99.99+%) and chromium-plated tungsten rods were obtained from Aldrich and R. D. Mathis, respectively. Test-grade silicon (100) wafers (Silicon Sense) were rinsed with ethanol (Pharmco) and dried in a stream of N_2 (BOC) prior to use in the evaporator. Distilled water was purified with a Millipore-Q system. Isooctane (J. T. Baker) and Na_2SO_4 (Mallinckrodt) were used as received. Octyl, dodecyl, and octadecyl thiols were obtained from Aldrich and purified by distillation or recrystallization before use. Docosyl,[4] hexadecyl,[4] and nonacosyl[5] thiols were available from previous studies, and eicosyl thiol[27] was synthesized via a literature procedure. 19-Octadecyloxy-1-nonadecanethiol,[28] 11-octadecyloxy-1-undecanethiol, 11-docosyloxy-1-undecanethiol, 19-docosyloxy-1-nonadecanethiol, and 22-docosyloxy-1-docosanethiol were available from previous studies.[11]

Sample Preparation. Copper samples were prepared by sequentially evaporating Cr and Cu at 1 and 12 Å/s, respectively, onto Si wafers in a diffusion-pumped chamber with a base pressure of 2×10^{-6} Torr. Immediately following the evaporation of copper, the chamber was backfilled with N_2, and the freshly evaporated samples were transferred under a positive flow of N_2 to deoxygenated, 0.5 mM isooctane solutions of ω-alkoxy-*n*-alkanethiols that were taken inside the evaporator. Polyethylene strips were placed around the circumference of the bell jar to reduce the effective area for air to enter the open chamber during the transfer. After remaining in solution for 1 h, the samples were removed, rinsed with isooctane and ethanol, and dried in a stream of N_2. The copper samples are polycrystalline and have a predominant (111) texture.[1]

Oxidation Studies. Immediately after assembly of the monolayers, the Cu-coated Si wafers were cut into 1.5×3 cm^2 samples that were either characterized or placed into a chamber at 100% relative humidity (RH). Humidity levels were determined by a digital hygrometer (Fisher). The chamber was evacuated and then backfilled with O_2 to atmospheric pressure. A steady stream of O_2 flowed through the chamber at 10 cm^3/min during the experiment. The chamber was kept at room temperature and stored in the dark to minimize any effects due to the possible influence of light. After various periods of exposure, samples were removed from the chamber, rinsed with water, dried in a stream of N_2, and characterized by IR, EIS, or XPS. After being characterized by EIS or XPS, the samples were discarded. Samples initially characterized by IR were often subsequently characterized by one of the other methods.

Electrochemical Impedance Spectroscopy (EIS). Electrochemical impedance spectroscopy of SAM-coated copper samples was performed with an EG&G 1025 frequency response detector connected to an EG&G 263A potentiostat, both interfaced to a personal computer. A glass cell equipped with a platinum mesh counter electrode and a Ag/AgCl/saturated KCl reference electrode contained an oxygenated solution of 0.050 M Na_2SO_4 as electrolyte. The electrolyte contacted only the center of the SAM-coated copper sample at an area of 1 cm^2 as confined by an O-ring. Corrosion potentials for each copper electrode were determined relative to the reference electrode by monitoring its potential at open-circuit over a few minutes in the oxygenated solution until an equilibrium potential was achieved. Impedance measurements were made in a three-electrode configuration at a set value of the measured corrosion potential with a 5 mV ac perturbation that was controlled between 10 mHz and 20 kHz. Film resistances and capacitances were determined by fitting the EIS data with an equivalent circuit[5] consisting of a solution resistance in series with a parallel combination of coating resistance and coating capacitance using software—Equivcrt.pas written by Bernard Boukamp—provided by EG&G.

Reflection−Absorption Infrared Spectroscopy (RAIRS). IR spectra were obtained in single reflection mode with a Bio-Rad FTS 175 infrared spectrometer and Universal Reflectance Attachment. The p-polarized light was incident at 80° from the surface normal, and the reflected light was detected with a narrow-band MCT detector. Spectral resolution was 2 cm^{-1} after triangular apodization. Spectra were referenced to those of SAMs prepared from octadecanethiol-d_{37} on copper with 1024 scans being acquired for both the sample and the reference. Integrated peak intensities were determined by fitting the spectra with Gaussian profiles.

Acknowledgment. We gratefully acknowledge financial support from the Arnold and Mabel Beckman Foundation, the MIT Sea Grant Program through a Henry and Grace Doherty Chair, and the MIT Undergraduate Research Opportunities Program (T.-H.Y. and J.C.M.).

JA020233L

(27) Bain, C. D.; Troughton, E. B.; Tao, Y.-T.; Evall, J.; Whitesides, G. M.; Nuzzo, R. G. *J. Am. Chem. Soc.* **1989**, *111*, 321−335.
(28) Xu, S.; Cruchon-Dupeyrat, S.; Garno, J. C.; Liu, G.-Y.; Jennings, G. K.; Yong, T.-H.; Laibinis, P. E. *J. Chem. Phys.* **1998**, *108*, 5002−5012.